Measurement of colloid concentration in drops using the time-shift technique

Lingxi Li*[1], Can Li[1, 2], Simon Rosenkranz[3], Walter Schäfer[3] and Cameron Tropea[1]

[1]Institute of Fluid Mechanics and Aerodynamics, Technische Universität Darmstadt, 64287, Darmstadt, Germany

[2]State Key Lab of Clean Energy Utilization, Zhejiang University, Hangzhou 310027, China

[3]AOM-Systems GmbH, 64646 Heppenheim, Germany

*Corresponding author: li@sla.tu-darmstadt.de

Abstract

This study is devoted to the measurement of colloid concentration in drops, as they occur in numerous industrial applications, such as paint sprays, ink-jet printing or the production of pharmaceutical products. A Monte Carlo ray-tracing approach has been used to study the light scattering from such particles, in which the polarization and intensity of all rays impinging onto a defined detector aperture are collected, allowing the signal generation arising from the drop passing through a plane wave or focused Gaussian beam to be simulated. When using a highly focused incident beam, the scattering corresponds to the optical arrangement of the time-shift technique, allowing the measurement of drops with suspended particles to be explored. For validation of the ray-tracing code, comparisons between the simulated time-shift signal and the measured time-shift signal were made, yielding excellent agreement. A model has been formulated to describe these signals; hence, to allow colloid concentration to be estimated directly from the received time-shift signals.

1. Introduction

Colloidal drops are encountered frequently in numerous process industries, such as in pharmaceutical products or spray drying to produce powders. However current optical measurements techniques are not capable of measuring the solid particle concentration in such drops [1]. The present study is devoted to the measurement of drop size and particle concentration of colloidal drops by using the time-shift technique [2]. This work builds on first results reported in [3], in which a Monte Carlo ray-tracing method was used to predict the time-shift signal received from "two-dimensional" drops. To simulate the photon transport in the colloidal drop by using the two-dimensional Monte Carlo method, the polarization state of the ray does not change after each scattering event; however, this is not the real case, because after each scattering event, not only the polar angle exhibits deviations, but also the azimuthal angle. This leads to a change of the polarization state. For the current simulation, a three-dimensional Monte Carlo ray-tracing code is developed in which the change of polarization state after each scattering event is considered. The polarization state of the ray is updated by tracking the reference plane. The outcome of this investigation is a recommendation of signal processing steps necessary to estimate solid particle concentration in drops from time-shift signals.

2. Colloidal drop model

In this section, the model for the colloidal drop is described. As Figure 1 illustrates, a drop with the diameter D contains a certain number of suspended particles, whose radius r is between the 0.1 λ to 5 λ; all particles have the same radius. Assuming a random distribution in space, the distance between two suspended particles in the drop follows the exponential distribution [4].
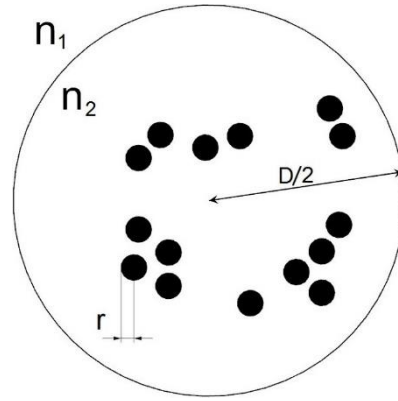
Figure 1: Drop with diameter D contains suspended particles with the radius of r. The refractive index for the surrounding medium and the drop is n_1 and n_2

Referring to Figure 1, the volume concentration of the colloids in the drop can be described as:

$$\kappa = \frac{N * V_p}{V_D} \tag{1}$$

in which N is the number of the suspended particles in the drop, and V_p and V_D are the volumes of a single suspended particle and the drop respectively. The optical average path length between scatterers *E(L)* is related to the concentration of colloidal particles, defined by the following equation [3]:

$$E(L) = \frac{V_p}{\kappa * \sigma_E} \tag{2}$$

in which σ_E describes the scattering cross section of the single suspended particle, assumed here to be $\sigma_E = \pi * r^2$.

3. Computational procedure

The light scattered from the surface of the drop is computed using an enhanced ray-tracing algorithm based on geometrical optics, as described in [5] and [6]. The geometric situation considered is a spherical drop with multiple suspended particles situated arbitrarily in the drop. For any ray intersecting the drop surface, the computation of the amplitude and the propagation direction of the reflected ray and transmitted ray follows the Fresnel equations and Snell's Law. For internal scattering, the ray path is computed using the Monte Carlo method. The ray path length between two consecutive scattering events is determined by the random free path length and the propagation direction. The computation process is described in the following two subsections.

3.1 Computation of the random free path length

The photon path is a series of straight segments between the consecutive scattering events, which is named the free path length. Its probability density distribution follows an exponential distribution [4]. After a ray travels the length *l*, the probability density function that the scattering event happens is given by:

$$P(l) = \frac{1}{E(L)} \cdot e^{-l/E(L)} \tag{3}$$

The cumulative distribution function follows that:

$$\int_0^{l_1} P(l) \cdot dl = \xi \tag{4}$$

Where ξ is a random number between (0, 1). Substituting equation (3) into (4), the relation between the free path length and ξ is obtained:

$$(1 - e^{-\frac{l_1}{E(L)}}) = \xi \tag{5}$$

$$l = -\ln(1 - \xi) * E(L) \tag{6}$$

Since ξ is between (0, 1), equation (4) can be expressed as [7]:

$$l = -\ln(\xi) * E(L) \tag{7}$$

Hence, in the Monte Carlo ray-tracing code, by generating a random number ξ between (0, 1), the random free path length can be determined with equation (7), whereby *E(L)* is given by the volume concentration (Eq. (2))

3.2 Computation of the new propagation direction of ray

A fundamental problem for the Monte Carlo simulation in three dimensions is the determination of the polar scattering angle and the azimuthal angle. The propagation direction of the ray should be updated after each scattering event, as well as the polarization state of the electric field. The scattering angle of the zenith angle and the azimuthal angle should be determined with the scattering phase function. When the size of colloidal particle is

between 0.2 λ and 10 λ, its scattering phase function can be described with Mie Theory [12]. The deflection of the scattering angle after the scattering event is illustrated in Figure 2.
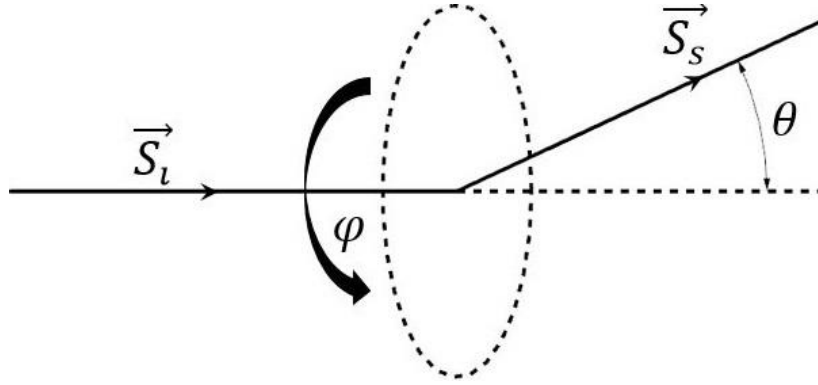

Figure 2: illustration for the polar deflection angle *θ* and azimuthal angle *φ* after the scattering event.

For the calculation of the polar deflection angle, the Henyey Greenstein phase function in Eq. (8) is used. The HG function describes the probability density for the deflection of the polar deflection angle. For the scattering in the azimuthal angle, the scattering is usually treated as isotropic. The azimuthal angle *φ* of scattering is uniformly distributed in [0, 2π].

$$HG(\theta) = \frac{(1 - g^2)}{(1 + g^2 - 2g(\cos\theta)^2)^{\frac{3}{2}}} \tag{8}$$

$$\varphi = 2\pi * \xi \tag{9}$$

where ξ is also a random number in the range $\in (0, 1)$ and g is the asymmetry factor that defines the distribution shape [8]. The factor g lies in the range $\in (-1, 1)$. g=1 means pure forward scattering; g=-1 means pure backward scattering: it can be expressed as the following:

$$g = \iint p(\vartheta) \cdot \cos\vartheta \, d^2\Omega \tag{10}$$

In which $p(\vartheta)$ is the phase function and follows:

$$\iint\limits_{4\pi} p(\vartheta) d^2\Omega = 1 \tag{11}$$

The cumulative distribution function of the equation (8) can be written as:

$$F_\theta(x) = \int_0^x HG(\theta) d\theta \tag{12}$$

where $x \in (0, \pi)$. There is no analytical expression for the inversion function of $F_\phi(x)$ [11]. Instead, the inversion function of cumulative probability density function of the cosine of polar deflection angle can be obtained directly. For the probability density function of the cosine of the polar deflection angle, its cumulative distribution can be written as:

$$F_c(x) = \int\limits_{-1}^x p(\cos(\theta)) d\cos(\theta) \tag{13}$$

For the distribution function $F_c(x)$, the inverse function can be expressed analytically [7]:

$$c_a(\theta) \stackrel{\text{def}}{=} \cos(\theta) = \begin{cases} \dfrac{1}{2g}\left(1 + g^2 - \left(\dfrac{1 - g^2}{1 - g + 2g\xi}\right)^2\right) & \text{if } g \neq 0 \\ 2\xi - 1 & \text{if } g = 0 \end{cases} \tag{14}$$

In the code, to determine the polar deflection angle and the azimuthal angle after the scattering event, two random numbers ξ_1 and ξ_2 are be generated and by using the equation (9) and (14), the polar deflection angle and the azimuthal angle can be determined.

For updating the direction after the scattering event, the new direction is calculated with the following equation [7]:

$$\begin{pmatrix} \hat{u}_x \\ \hat{u}_y \\ \hat{u}_z \end{pmatrix} = \begin{bmatrix} \dfrac{u_x * u_z}{\sqrt{1-u_z{}^2}} & -\dfrac{u_y}{\sqrt{1-u_z{}^2}} & u_x \\ \dfrac{u_y * u_z}{\sqrt{1-u_z{}^2}} & -\dfrac{u_x}{\sqrt{1-u_z{}^2}} & u_y \\ -\sqrt{1-u_z{}^2} & 0 & u_z \end{bmatrix} \cdot \begin{pmatrix} \sin\theta\cos\varphi \\ \sin\theta\sin\varphi \\ \cos\theta \end{pmatrix} \tag{15}$$

In which, the $[u_x ,\ u_y ,\ u_z]$ represent the current direction and the $[\hat{u}_x ,\ \hat{u}_y ,\ \hat{u}_z]$ is the direction after the scattering event. After the calculation of the new direction, the polarization state of the electric field should also be updated.

With the initial position, the free path length, and the propagation direction, the position and the propagation direction after the scattering event can be calculated. The computation procedure for the single ray is explained with the flow chart in Figure 3. For the single ray, the ray tracing inside the drop will be terminated when its intensity is less than 1% of the original intensity.
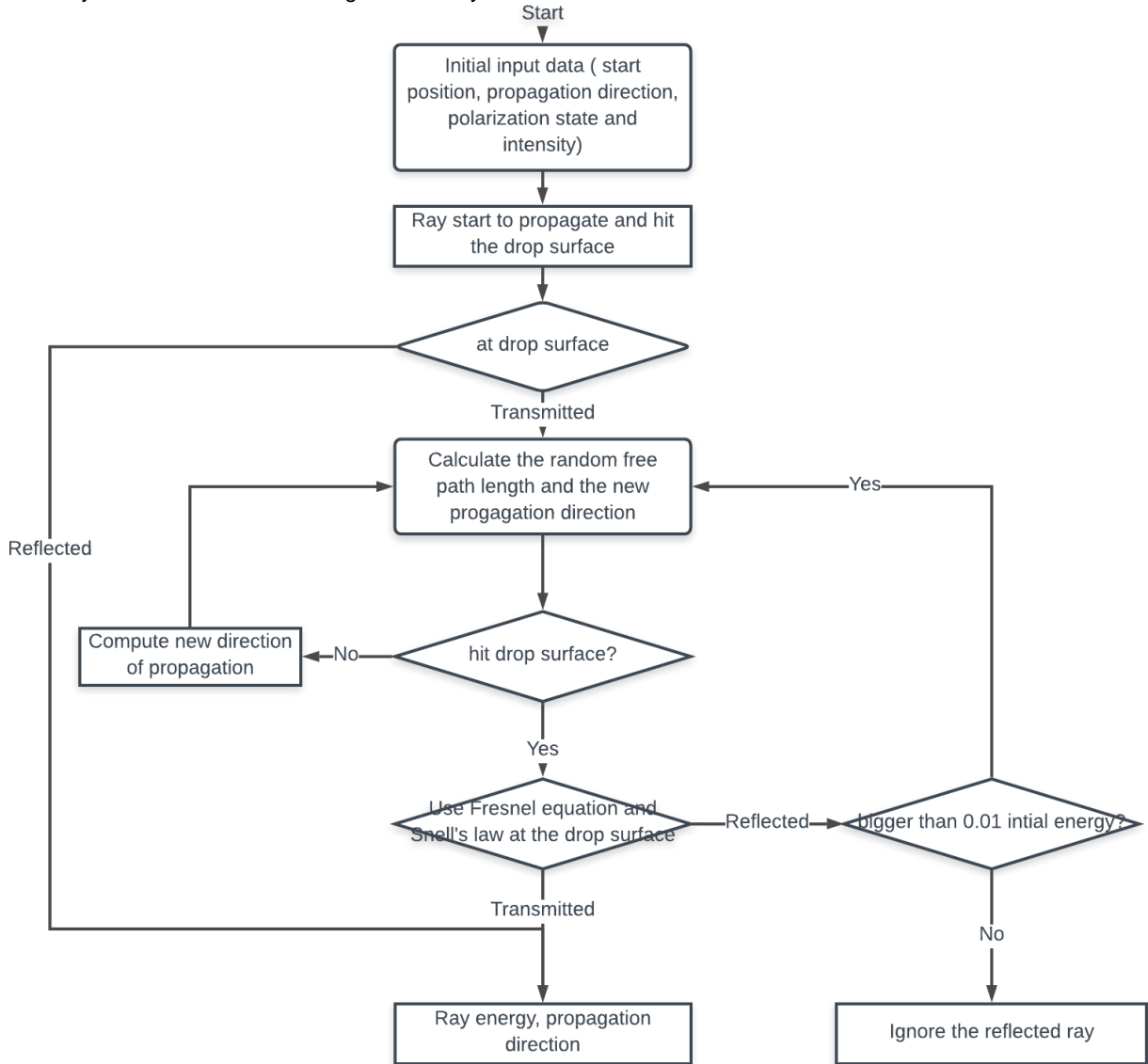

Figure 3: Flow chart for the computation procedures for the single ray by using the Monte Carlo method

For each computation of the time-shift signal, several millions of rays were launched into the colloidal drop to build up the time-shift signal. The computation procedure in the Figure 3 is repeated for all the rays. The scattered intensity is the intensity sum of all rays impinging onto the detector surface. All rays are treated completely incoherent, and the intensity of individual rays is first computed. If M stands for the number of the rays which falls onto the prescribed detector aperture, the total received intensity is given by equations (16) and (17) [5]:

$$I_k = \frac{c}{2}|\boldsymbol{E}|^2 \tag{16}$$

$$I_{total}(\theta_i, \varphi_j) = \sum_{k=1}^{M} I_k \qquad (17)$$

4. Simulated signal for the time-shift technique

The time-shift technique, which is also known as the pulsed-displacement technique, is a method to measure size, velocity, and relative refractive index (m) of spherical particles. As Figure 4 illustrates, two detectors placed in the backscattering direction (e.g. 160°) will register a time dependent signal comprising several peaks, as illustrated in the Figure 4, corresponding to the different scattering orders when a transparent drop passes through a shaped beam. Details about the measurement principle and optical design can be found in [2], [9], [10]. When the drop passes through the laser beam, typically for each detector, three signal peaks are obtained. The signal peaks are designated *p=0*, which is obtained from the reflection scattering, *p=2.1* and *p=2.2*, which are obtained from second-order refraction scattering.
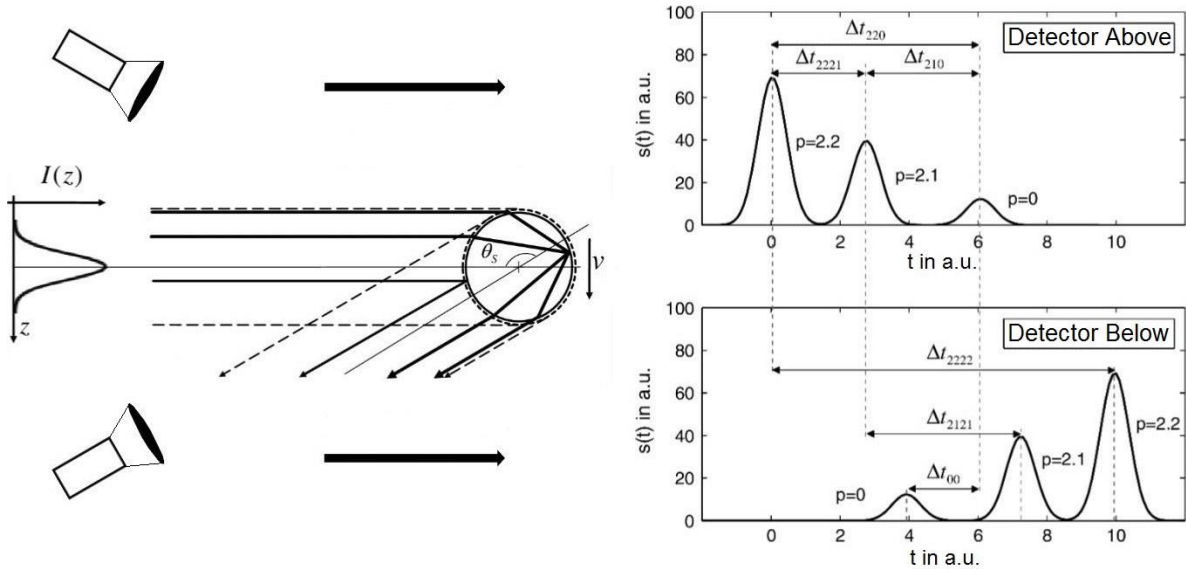

Figure 4: Principle of time-shift measurement technique, adapted from [2]. θ_s expresses the angle of the incident point for each scattering order.

4.1. Simulated time-shift signal for water drop

For simulation, certain specific values have been fixed to match the arrangement of the real measurement instrument: the beam waist of the laser source is 8 µm; a detector is place at the scattering angle 165° with a solid angle of 0.032 sr.; the laser source is perpendicularly polarized with the wavelength 405 nm.

First, the time-shift signal for a pure water drop is simulated. The water drop is generated with a monodispersed droplet generator (FMP, Erlangen) with a diameter of 120µm, as Figure 5 (a) shows. Figure 5 (b) shows the results for the comparison between the simulated time-shift signal and the measured time-shift signal. In Figure 5 (b), the black dashed line represents the simulated time-shift signal; the blue solid line is the measured signal from the experiment: the agreement is satisfactory.
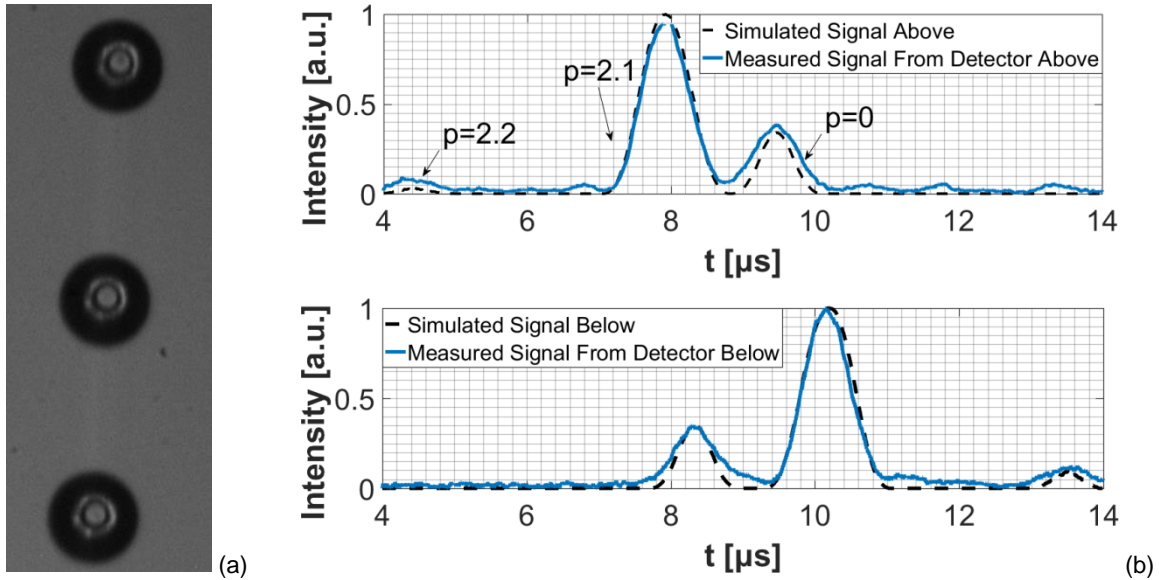
(a)

(b)

Figure 5: (a) Drop chain with a diameter of 120µm generated by a FMP droplet generator; (b) Comparison between the simulated time-shift signal and the measured time-shift signal for a water drop with the diameter 120µm. (Scattering angle $\theta_s=165°$, s polarization)

4.2 Simulated time-shift signal for colloidal drop

The time-shift signals have been simulated for a colloidal drop by varying the volume concentration. The drop size is 100 µm with a relative refractive index of $n_2=1.34$. The volume concentration is about 4% and 8 %, which correspond to optical average path lengths of 20µm and 10µm.

(a). *Time-shift signal for E(L)=20µm*

(b). *Time-shift signal for E(L)=10µm*

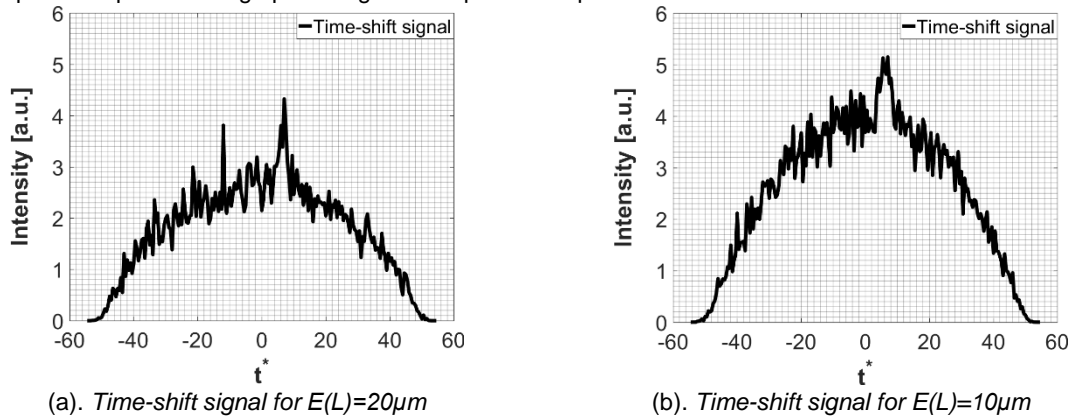**Figure 6: Simulated time-shift signals from the colloidal drop for optical average path length $E(L)=20µm$ and $E(L)=10µm$. ($D_{Drop}=100µm$, $\theta_s=165°$, p polarization)**

Figure 6 shows the simulated time-shift signals from one detector for the $E(L)=20µm$ und $E(L)=10µm$ separately. Both of the signals exhibit the feature that a signal peak sits on a pedestal. The pedestal arises through the internal scattering from the suspended particles and the signal peak arises from the reflection scattering from the drop surface. Comparing the results in Figure 6 (a) and (b), the reflection peaks have a similar height; this is because the suspended particle does not affect the reflection from the surface and furthermore, the reflection peak should have the same amplitude as the reflection peak from a pure drop with the same size. However, the signal height from the internal scattering is different. When the optical average path length is larger, this corresponds to a smaller volume concentration of solid particles in the drop. Therefore, the internal scattering from the drop with $E(L)=20µm$ is weaker than the internal scattering from drop with $E(L)=10µm$. Hence, the ratio between the amplitude of the reflection peak S_r and the remaining signal pedestal strength S_w is related to the optical average path length of the colloidal drop. For a given size of the droplet, a look-up table for the relationship between this ratio and the optical average path length of the colloidal drop could be created.

5 Signal processing

The optic arrangement of the time-shift measurement instrument is illustrated in Figure 4, in which the detector covers a solid angle of 0.032 sr. When a pure drop falls through a Gaussian beam, the Generalized Lorenz-Mie Theory [13] predicts a scattered intensity in the far-field as [14]:

$$I(r, \theta, \varphi) = \frac{1}{2\mu_0 c k^2 r^2} \left[|S_1(\theta_D, \varphi_D)|^2 + |S_2(\theta_D, \varphi_D)|^2 \right] \tag{17}$$

in which S_1 and S_2 are the scattering amplitudes for parallel and perpendicular polarized Gaussian beam separately; θ_D and φ_D are the polar angle and azimuthal angle of the detector center in the spherical coordinate system; k is the wave number.

When a colloidal drop passes through the laser beam, a signal, which is similar to the signal in Figure 6, will be detected by the detector. The size of the drop can be determined as the time shift between the two reflection peaks [2]. By integrating equation (17) over the detector surface, the amplitude of reflection peak S_r can be computed. Then the ratio between the amplitude of the reflection peak S_r and the remaining signal pedestal S_w could be obtained. With the look-up table, the optical average path length of the colloidal drop could be estimated, and then the volume concentration of the particles could be calculated using equations (1) and (2).

Discussion and Conclusions

In the study, a three-dimensional Monte Carlo ray-tracing model is developed to predict the time-shift signal from a colloidal drop, which builds on the work from [3]. For validation, the simulated time-shift signal has been compared with the measured time-shift signal from the pure drop, yielding excellent agreement. It's clear that the current work is still limited to the measurement of solid particle concentration in the colloidal particle. For the further work, the results from the simulation will be compared with the results from simulated results by using the discrete dipole approximation method [15] and the results from corresponding experiments.

Acknowledgements

References

[1]. Tropea C., Optical particle characterization in flows, Ann Rev Fluid Mech 43:399-426 (2011).
[2]. Schäfer W., Tropea C., Time-shift technique for simultaneous measurement of size, velocity and relative refractive index of transparent droplets or particles in a flow, Appl Optics 53:588-596 (2014).
[3]. Rosenkranz S., Schäfer W., Tropea C., Zoubir A.M., Modeling photon transport in turbid media for measuring colloidal concentration in drops using the time-shift technique, Appl Optics 55:9703-9711 (2016).
[4]. Feller W., **An Introduction to Probability Theory and Its Applications**, Vol. I. Wiley, London (1950).
[5]. Li L., Rosenkranz S., Schäfer W., & Tropea C, Light scattering from a drop with an embedded particle and its exploitation in the time-shift technique. J Quant Spectr Radiat Transfer, 227:20-31 (2019).
[6]. Stegmann P.G., Tropea C., Järvinen E., Schnaiter M., Comparison of measured and computed phase functions of individual tropospheric ice crystals, J Quant Spectr Radiat Transfer 178:379-389 (2016).
[7]. Berrocal E., Meglinski I. and Jermy M, New model for light propagation in highly inhomogeneous polydisperse turbid media with applications in spray diagnostics. Optics Express, 13(23), pp.9181-9195 (2005).
[8]. Wendisch M., Yang P., **Theory of Atmospheric Radiative Transfer: A Comprehensive Introduction**. John Wiley & Sons, Weinheim (2012).
[9]. Hess C.F., Wood C.P., Pulse displacement technique to measure particle size and velocity in high density application, In Laser Techniques and Applications to Fluid Mechanics, Adrian R.J., Durao D., Durst F., Heitor M.V., Maeda M., Whitelaw J.H., (eds.) Springer-Verlag, Berlin, Germany, 131-144 (1993).
[10]. Albrecht H.E., Damaschke N., Borys M. and Tropea C., **Laser Doppler and Phase Doppler Measurement Techniques**. Springer Science & Business Media, Heidelberg, (2013).
[11]. Żołek N. S., Wojtkiewicz S., & Liebert A. Correction of anisotropy coefficient in original Henyey Greenstein phase function for Monte Carlo simulations of light transport in tissue. Biocybernetics and Biomedical Engineering, 28(4), 59-73 (2008).
[12]. Mie G., Beiträge zur Optik trüber Medien, speziell kolloidaler Metallösungen. Annalen der Physik, 330(3), pp.377-445 (1908).
[13]. Gouesbet G. and Gréhan G., **Generalized Lorenz-Mie Theories** (Vol. 31). Springer, Berlin (2011).
[14]. Lock J.A., Improved Gaussian beam-scattering algorithm. Applied optics, 34(3), pp.559-570 (1995).
[15]. Yurkin M.A. and Hoekstra A.G., The discrete dipole approximation: an overview and recent developments. J Quant Spectr Radiat Transfer, 106(1-3), pp.558-589 (2007).